Chapter

# Binary Metal Oxides Thin Films Prepared from Pulsed Laser Deposition

*Cyril Robinson Azariah John Chelliah and Rajesh Swaminathan*

## Abstract

The semiconductor industry flourished from a simple Si-based metal oxide semiconductor field effect transistor to an era of MOSFET-based smart materials. In recent decades, researchers have been replacing all the materials required for the MOSFET device. They replaced the substrate with durable materials, lightweight materials, translucent materials and so on. They have came up with the possibility of replacing dielectric silicon dioxide material with high-grade dielectric materials. Even then the channel shift in the MOSFET was the new trend in MOSFET science. From the bulk to the atomic level, transistors have been curiously researched across the globe for the use of electronic devices. This research was also inspired by the different semiconductor materials relevant to the replacement of the dielectric channel/gate. Study focuses on diverse materials such as zinc oxides (ZnO), electrochromic oxides such as molybdenum oxides (including $MoO_3$ and $MoO_2$) and other binary oxides using ZnO and $MoO_3$. The primary objective of this research is to study pulsed laser deposited thin films such as ZnO, $MoO_3$, binary oxides such as binary ZnO /$MoO_3$, ZnO /$TiO_2$ and ZnO/$V_2O_5$ and to analyse their IV properties for FET applications. To achieve the goal, the following working elements have been set: investigation of pulsed laser deposited thin film of metal oxides and thin film of binary metal oxide nanostructures with effects of laser repetition and deposition temperatures.

**Keywords:** binary oxides, PLD, thin film, metal oxides

## 1. Introduction

Metal oxide thin film plays an important role in various applications such as aircraft cockpits, electronic displays, medical devices, solar panels, smart windows and high-temperature sensors in spacecraft, photonics, photodetectors, infrared detectors, phototransistors, transparent electronics, optics, anti-reflective and decorative coatings [1]. They own excellent banding and carrier mobility for conduction phenomena in the field effect transistor application. The semiconductor industry flourished from a simple Si-based metal oxide semiconductor field effect transistor to an era of MOSFET-based smart materials. In recent decades, researchers have been replacing all the materials needed for the MOSFET unit. They replaced the substrate with flexible materials, light weight material, transparent

material, etc. They also come up with the idea of replacing dielectric silicon dioxide material with high-grade dielectric materials. And changing the channel in the MOSFET has become the latest trend in FET research. From the bulk to the atomic level, transistors have been interestingly studied around the globe for the application of electronic devices. This research was therefore motivated by the various semiconductor materials applicable to the replacement of the dielectric channel/gate [2, 3].

Research focuses on various materials such as zinc oxides (ZnO), electrochromic oxides such as molybdenum oxides (including $MoO_3$ and $MoO_2$) and various binary oxides using ZnO and $MoO_3$. New electrical results are studied with the investigation of the conduction mechanism using ac complex impedance spectroscopy with ZnO and $MoO_3$ binary oxides. This has motivated the research to work on new binary materials with ZnO /$TiO_2$ and ZnO /$V_2O_5$. As a result, we investigated the various electrical properties and complex impedance parameters using ac impedance spectroscopy. An attempt with pulsed laser deposited ZnO thin film as a channel layer and $Al_2O_3$ as a dielectric layer in FET was fabricated and studied. A transistor with ZnO channel, $MoO_3$ as an interlayer with source-substrate and drain-substrate, and a layer of binary oxides ZnO/$MoO_3$ and $ZrO_2$ as a dielectric stack layer is also manufactured and analysed.

The primary objective of this research is to study the pulsed laser deposited thin films such as ZnO, $MoO_3$, binary oxides such as ZnO/$MoO_3$, ZnO/$TiO_2$ and ZnO/$V_2O_5$ and their behaviour as gate dielectric layer to investigate the IV properties for FET applications. To achieve the objective following work elements were set: First to investigate the pulsed laser deposited thin films of ZnO nanostructures with the effects of laser repetition rate and deposition temperatures, then an investigation of the $MoO_3$ and $MoO_2$ thin films by pulsed laser deposition with the impact of $O_2$ and Ar atmosphere gas and deposition temperatures. The research continued its next set of investigation of the current conduction mechanism of the pulsed laser deposited binary oxide ZnO/$MoO_3$, ZnO/$TiO_2$ and ZnO/$V_2O_5$ thin films using ac complex impedance spectroscopy and the impact of wide range of temperature from 298 K to 423 K and a wide range of frequency from 1 Hz to 1 MHz. Finally, a ZnO thin film by pulsed laser deposition as n-channel MOSFET and its performance of ZnO channel along with various binary oxides and interlayer $MoO_3$ in MOSFET were studied [4].

## 2. Materials and methods

### 2.1 General information on zinc oxide

Zinc oxide is a unique material that exhibits exceptional semiconducting, piezoelectric, and pyroelectric properties. Nanostructures of ZnO are equally as important as carbon nanotubes and silicon nanowires for nanotechnology and have great potential applications in nanoelectronics, optoelectronics, sensors, field emission, light-emitting diodes, photocatalysis, nanogenerators, and nanopiezoelectronics. Fundamental understanding about the growth of ZnO nanowires is of critical importance for controlling their size, composition, structure, and corresponding physical and chemical properties [5].

### 2.2 General information on transition metal oxide

Moreover, the $MoO_3$, $V_2O_5$ and $TiO_2$ belong to the transition metal oxides (TMO) family. Hence these mixed metal oxides $MoO_3$, $V_2O_5$ and $TiO_2$ also called as binary

transition metal oxides (BTMOs). They consist of at least one transition metal ion and one or more electrochemically active/inactive ions. They can use the synergism behavior of pure oxides, which can enrich the capacitive performance with an expanded potential window, supplementary active sites, excellent conductivity and improved stability. According to Zhang et al. [6], BTMOs possess higher reversible capacity, better structural stability and electronic conductivity, and have been widely studied to be novel electrode materials for transistor applications.

### 2.3 Basic properties of ZnO, $MoO_3$, $TiO_2$ and $V_2O_5$

**Table 1** provides the basic properties of ZnO, $MoO_3$, $TiO_2$ and $V_2O_5$.

### 2.4 Pulsed laser deposition

The various thin film deposition methods are sol–gel deposition, thermal electrodeposition, chemical vapor deposition, sputtering, atomic layer deposition, pulsed laser deposition and so on. Among these the pulsed laser deposition is a sophisticated, rich and excellent deposition method especially for metal oxides (MO) thin films depositions.

### 2.5 Physical principle

A pulsed laser beam is allowed to hit the target material which is placed on the target holder. This is fixed with the rotating target carrousel. A laser plume consisting of atoms, molecules, ions, nanoparticles and microparticles also known as plasma produced. This plasma of molten material by the pulsed laser starts

| **Properties** | **Zinc oxide** | **Molybdenum oxide** | **Titanium dioxide** | **Vanadium pentoxide** |
|---|---|---|---|---|
| Molecular formula | ZnO | $MoO_3$ | $TiO_2$ | V2O5 |
| Molar mass (g/mol) | 81.39 | 143.94 | 79.87 | 149.88 |
| Appearance | White solid | Colorless or white to slightly bluish powder or granules | White powder | Yellow to red crystalline powder |
| Odor | Odorless | Odorless | Odorless | Odorless |
| Density ($g/cm^3$) | 5.61 | 4.70 | 4.23 | 3.36 |
| Refractive index | 2.0041 | 2.5166 | 2.9103 | 2.3 |
| Melting point | 2248 K (decomposes) | 1068 K | 2128 K | 2213 K |
| Boiling point | 2633 K | 1428 K (sublimes) | 3273 K | 2023 K (decomposes) |
| Solubility in water | 0.16 mg/100 mL (at 30 °C) (Insoluble in water) | 0.49 g/1000 mL in water at 28 °C | Insoluble in water | 1 g / 125 mL (slightly soluble) |
| Bandgap (eV) | 3.34 (direct) | 2.9 (direct) | 3.2 (indirect) | 2.8 (indirect) |
| Dielectric constant | 8.33 | 35 | 80 | 37.2 |
| CAS number | 1314-13-2 | 1313-27-5 | 13463–67-7 | 1314-62-1 |

**Table 1.**
*Basic properties of the ZnO, $MoO_3$, $TiO_2$ and $V_2O_5$.*

depositing on the substrate a rich, vibrant, stoichiometric and neatly arranged self-assembled layers. **Figure 1** depicts the schematic of the working principle of the PLD.

### 2.6 Working operation of PLD

**Figure 2(a)** and **(b)** shows the flowchart of the experiments to be carried out in a standard procedure before and after the deposition process using the pulsed laser deposition system.

### 2.7 Advantages of using PLD

The advantages of using PLD include:

i. wavelength and power density flexibility help to ablate any material combination.

ii. laser system is separated from the vacuum system hence while in the ablation geometry there is a considerable degree of freedom

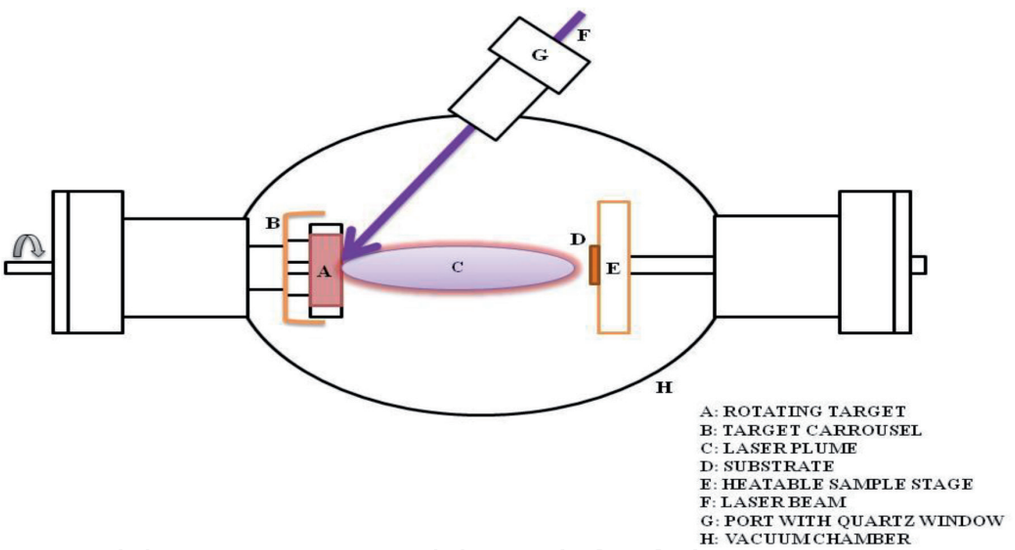


**Figure 1.**
*Schematic working of pulsed laser deposition.*

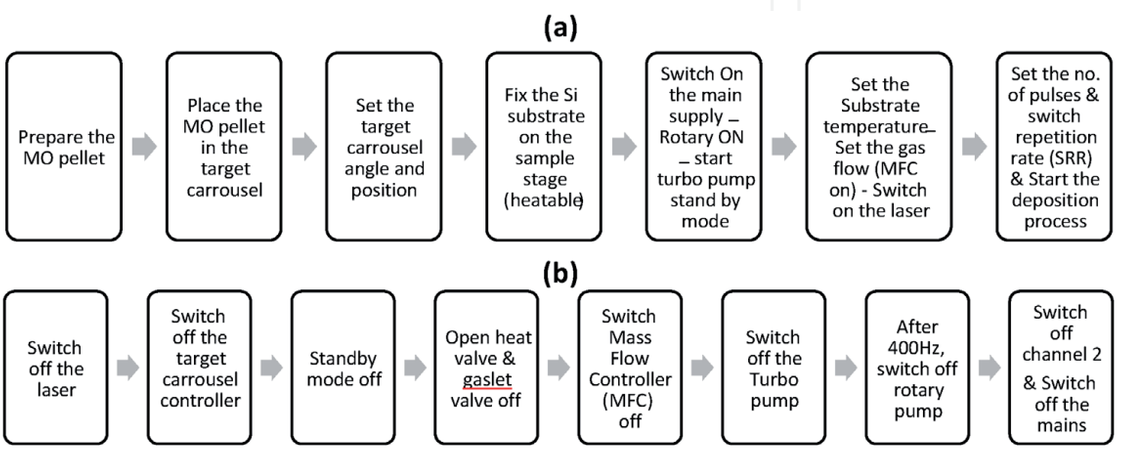


**Figure 2.**
*Operation of PLD instrument (a) before and (b) after deposition.*

iii. a precise control over the growth rate is enabled by the usage of laser beam and

iv. the transfer of the composition for most of the ablated materials show better congruence and stoichiometry.

## 3. Experimental details

**Figure 3** shows the schematic of ZnO deposited on Si/glass substrate by pulsed laser deposition. In this work, pulsed laser deposition technique was used for growing high quality stoichiometric ZnO thin films. Laser from the source hits the ZnO target, a plasma plume consisting of molecules and atoms of zinc and oxygen start to deposit on the surface of the substrate. The plasma plume regime is known as the plasma perimeter. Mostly the plume will be centered in the course of the plasma perimeter. The plasma perimeter dependent upon the factors such as laser energy, laser repetition rate, temperature maintained, pressure and the distance between the target and the substrate. A detailed study of the effects of laser repetition rate, deposition and annealing temperatures on the electrical, optical and structural properties of the pulsed laser deposited ZnO thin films were carried out.

In the same way the preparation for other materials such as $MoO_3$, $MoO_2$, binary oxides $ZnO/MoO_3$, $ZnO/TiO_2$ and $ZnO/V_2O_5$ were carried out with pulsed laser deposition. Various analytical techniques such as SEM, UV–Visible spectroscopy, current–voltage characterization, ac complex impedance spectroscopy were also carried out to study the structural, morphological, optical and electrical properties.

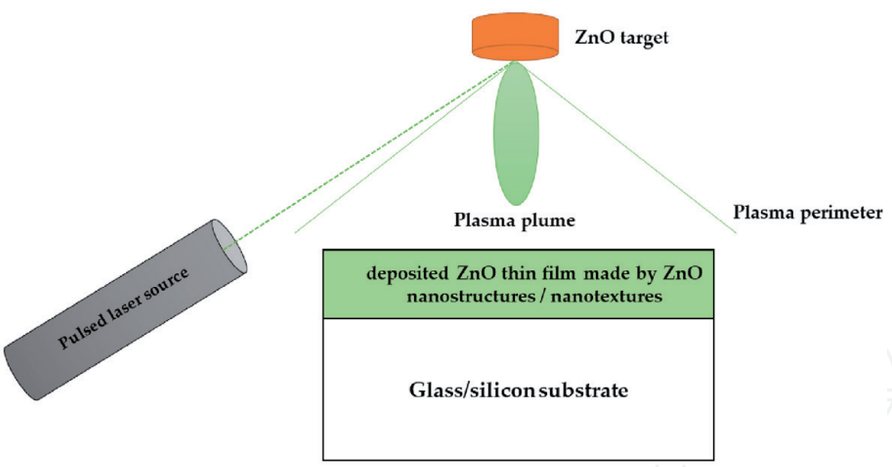


**Figure 3.**
*Schematic of pulsed laser deposited ZnO thin film nanostructures/nanotextures on Glass/Si substrate [7].*

## 4. Results and discussion

### 4.1 Investigation of ZnO nanostructures with the effects of laser repetition rate and deposition temperatures

The structure and properties of the transparent ZnO films deposited on glass substrates were then analyzed using X-ray Diffraction (XRD) as shown in **Figure 4** and confirmed the presence of hexagonal wurzite ZnO for the samples deposited at 300 °C, 450 °C and 600 °C [8].

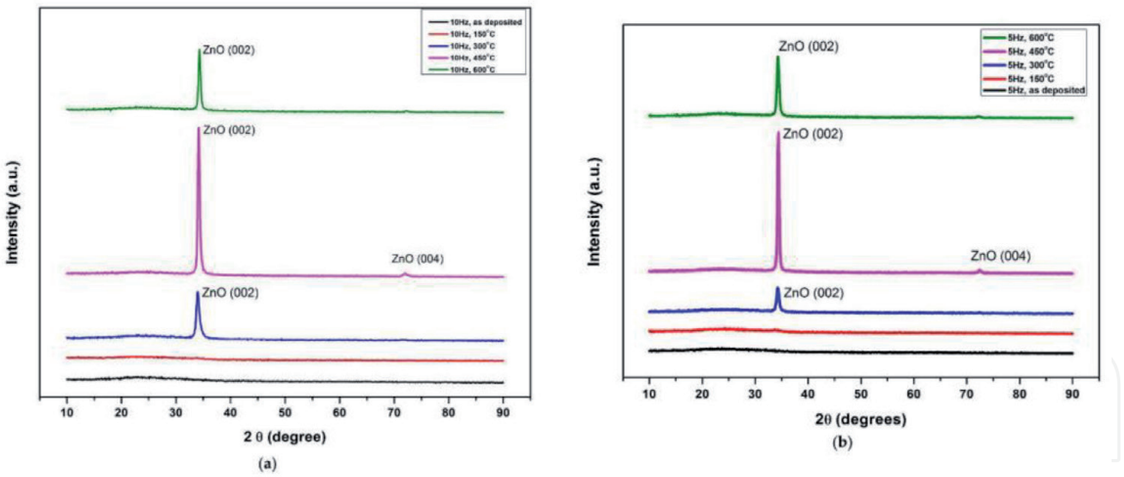


**Figure 4.**
*XRD spectra of ZnO thin films (a) 10 Hz samples and (b) 5 Hz samples - (i) as deposited, (ii) at 150 °C, (iii) at 300 °C, (iv) at 450 °C and (v) at 600 °C.*

It is also confirmed by the card no. 80–0074 of the Joint Committee on Powder Diffraction Standards (JCPDS) [9]. The XRD results provide the wurzite hexagonal crystal structure for the sample deposited at the temperature from 300-450 °C. The high intensity (002) plane preferentially grows in thin films above 300 °C. The (002) peaks become intense if the substrate temperature is increased from 300 to 600 °C. The grain size of the polycrystalline film increased with increasing the substrate temperature while deposition. **Table 2** provides the details of the bandgap energy calculated from the UV transmission spectra of the sample at various temperatures such as 25 °C (as deposited), 150 °C, 300 °C, 450 °C and 600 °C samples.

The transmission spectra for 10 Hz and 5 Hz samples are shown in **Figure 5**.

The ZnO thin films deposited at 10 Hz and 5 Hz shows an excellent transmittance and high transparency rate along with a decreasing energy bandgap as the temperature increases from as deposited sample at room temperature to 450 °C. The value of bandgap is estimated from fundamental absorption edge of the films. For the direct transitions, the absorption coefficient is expressed by

$$(\alpha h\nu)^2 = k\left(h\nu - E_g\right) \quad (1)$$

where k is constant, $E_g$ is the energy bandgap, $\nu$ is the frequency of the incident radiation and h is Planck's constant. Because ZnO has a large exciton binding energy of 60 meV, an obvious exciton effect will always appear in the absorption spectra of high-quality ZnO films. As the ZnO thin film quality improves, a pronounced exciton absorption peak located at 3.1–3.3 eV was observed. The UV band was

| Samples | UV emission center at 10 Hz (nm) | Bandgap energy (eV) | UV emission center at 5 Hz (nm) | Bandgap energy (eV) |
|---|---|---|---|---|
| As deposited | 399 nm | 3.209 | 400 nm | 3.218 |
| 150 °C | 395 nm | 3.177 | 395 nm | 3.177 |
| 300 °C | 393 nm | 3.161 | 394.8 nm | 3.176 |
| 450 °C | 393 nm | 3.161 | 393.5 nm | 3.165 |
| 600 °C | 409 nm | 3.290 | 394.3 nm | 3.172 |

**Table 2.**
*Bandgap energy of the samples deposited at various temperatures obtained from UV transmission spectra.*

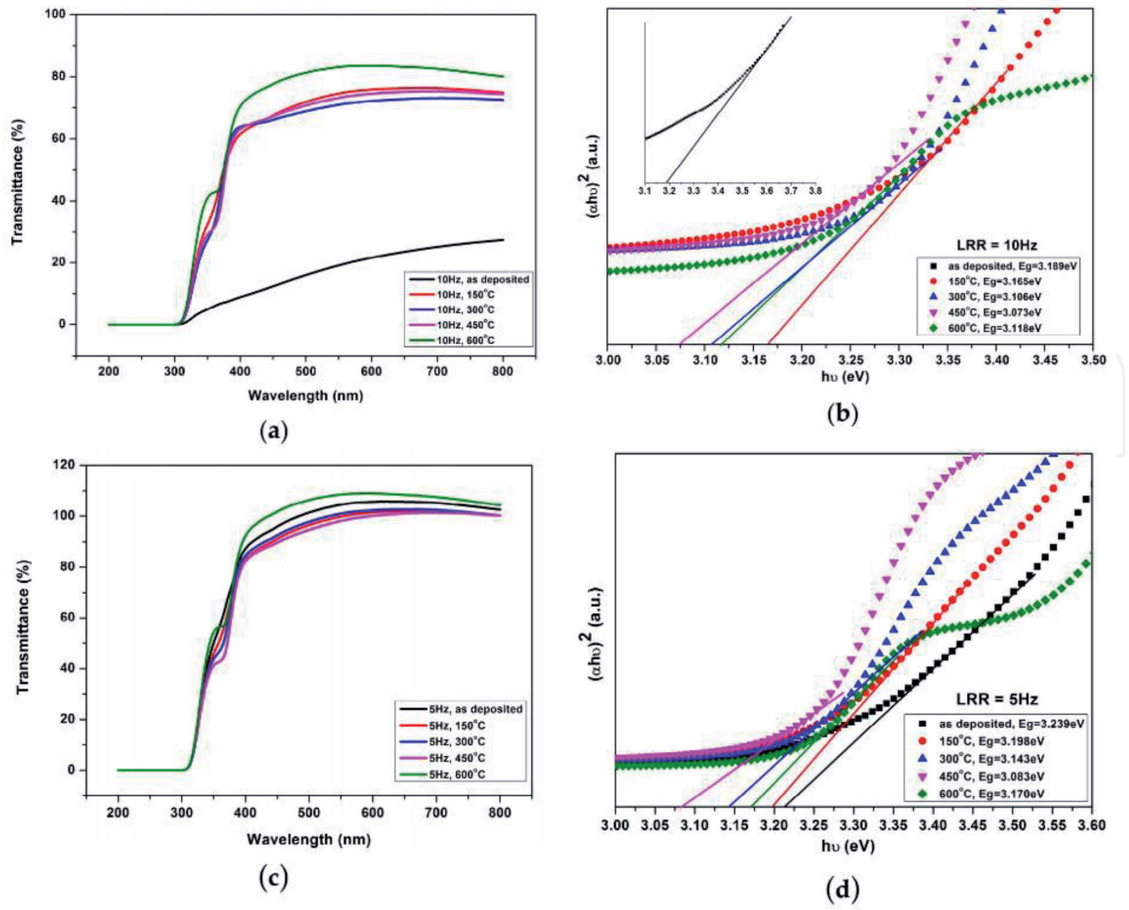


**Figure 5.**
*UV-Transmittance (T%) spectra at various deposition temperatures (a) Wavelength Vs T% of 10 Hz samples, (b) Tauc-plot of 10 Hz samples (c) Wavelength Vs T% of 5 Hz samples and (d) Tauc-plot of 5 Hz samples.*

assigned to be the free exciton. It is also observed that at 600 °C the energy bandgap started to increase slightly. The bandgap energies obtained from Tauc-plot of optical transmittance are tabulated in **Table 3**.

### 4.2 Investigation of $MoO_3$ and $MoO_2$ nanostructures

**Figure 6** shows the FESEM images of the pulsed laser deposited with various thin film of molybdenum oxide. The sample deposited at 450 °C and using the $O_2$ gas atmosphere, near the edges and unfilled region, hexagonal (100) nanotubes, along with neatly arranged orthorhombic (040) molybdenum trioxide ($MoO_3$) structures is shown in **Figure 6a**. Followed with **Figure 6b** shows the sample deposited at 450 °C using the $O_2$ gas atmosphere, uniformly arranged orthorhombic (040) structures of the $MoO_3$ seen. Then, **Figure 6c** shows the sample stored at

| Samples | $E_g$ at 10 Hz (eV) | $E_g$ at 5 Hz (eV) |
|---|---|---|
| As deposited | 3.189 | 3.239 |
| 150 °C | 3.165 | 3.198 |
| 300 °C | 3.106 | 3.143 |
| 450 °C | 3.073 | 3.083 |
| 600 °C | 3.118 | 3.170 |

**Table 3.**
*Bandgap energy obtained from Tauc plot of optical transmittance.*

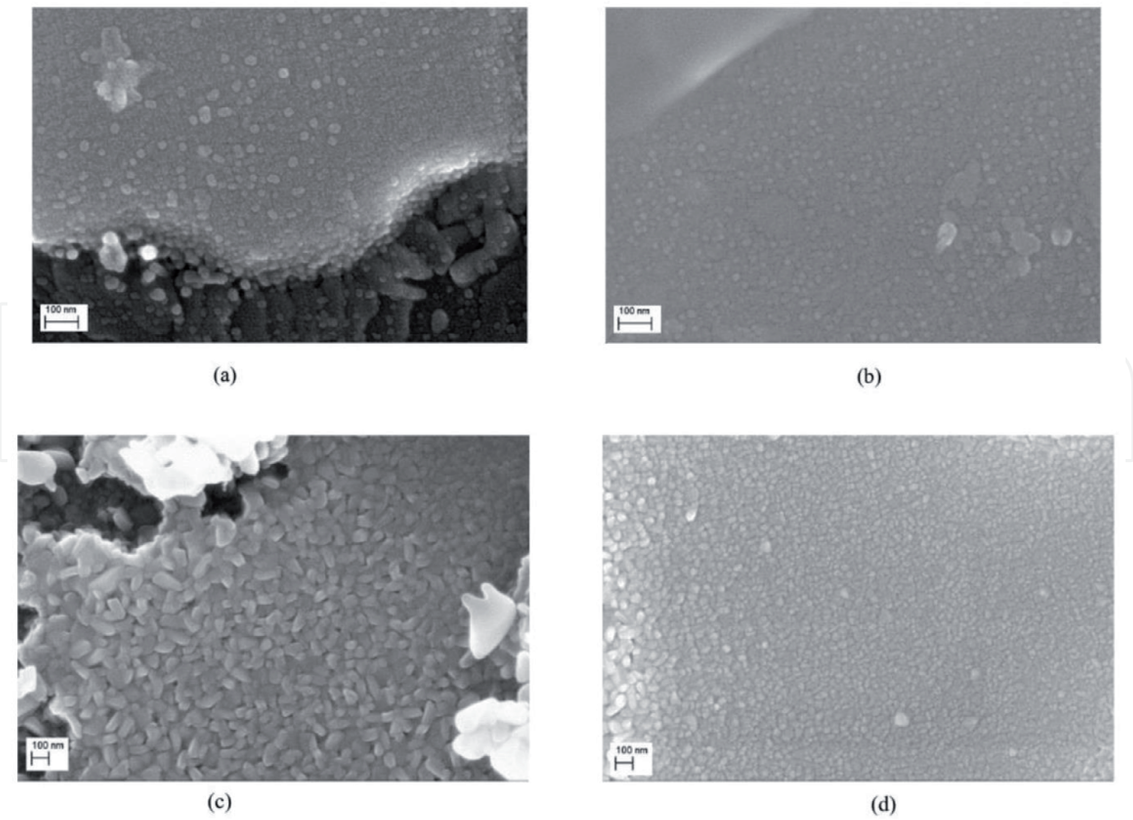


**Figure 6.**
*Field Emission Scanning Electron Microscopy (FESEM) images of molybdenum oxides thin films deposited by PLD. (a) and (b) $MoO_3$ at 450 °C (c) and (d) $MoO_2$ at 450 °C.*

450 °C under the argon gas atmosphere, near the unfilled region, neatly arranged monoclinic molybdenum dioxide ($MoO_2$) structures. Finally, the sample deposited at 450 °C using the argon gas atmosphere, which shows uniformly arranged monoclinic $MoO_2$ structures is shown in **Figure 6d** [10].

**Figure 7** shows the XRD spectra of the pulsed laser deposited molybdenum oxide thin films at the various conditions. The sample deposited at the room temperature was the as-deposited thin film which exhibits the amorphous nature. Then the sample was deposited at a substrate temperature of 450 °C and 600 °C, which exhibit orthorhombic structure with 020 and 040 peaks and are confirmed with the ICSD 80577. Then the deposition duration was increased from 2 minutes to 20 minutes, with the $O_2$ atmosphere, which results in orthorhombic structures and hexagonal structures and the peaks are found at 100 and 211 respectively. Then the next sample when deposited with same temperature and duration under the Ar atmosphere, the XRD spectra shows the monoclinic structures and confirms as in **Figure 4** the presence of $MoO_2$ with 110, 020 and 220 peaks with the ICSD 23722 and JCPDS 65–5787. When the sample deposition temperature increased from 450 °C to 600 °C, the structure crystallization takes place [11].

### 4.3 Investigation of conduction mechanism by ac complex impedance spectroscopy for PLD binary oxides ZnO/$MoO_3$ thin films

The complex impedance (Z" vs. Z') plots of pulsed laser deposited binary oxides ZnO/$MoO_3$ (ZMO) thin films are displayed in **Figure 8**. The response of a measurement in a complex impedance plot enables us to separate two contributions which appear in the form of semicircles arcs. We know that, for a semiconducting material having interfacial boundary layers (grain-boundary) and the figure exhibits

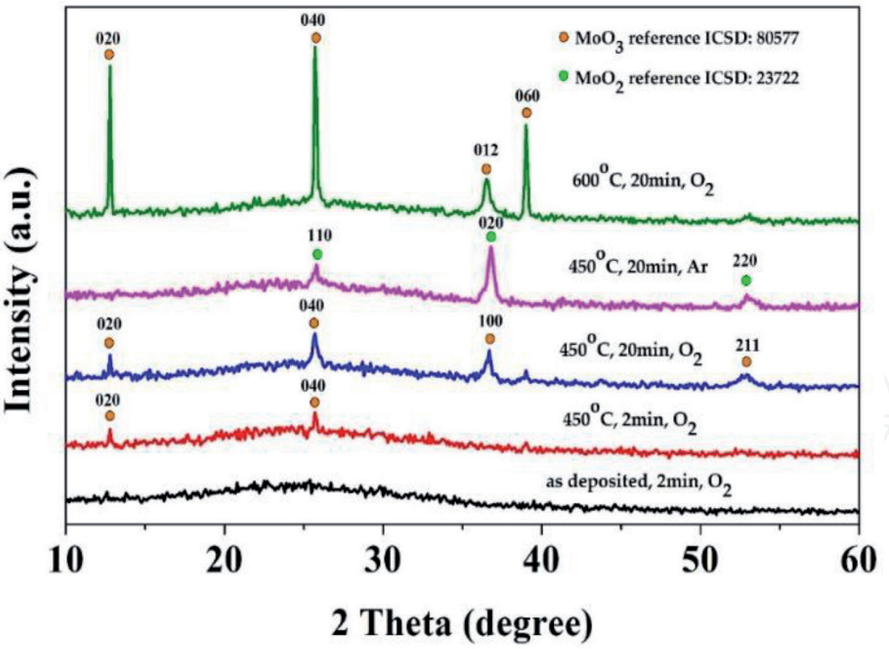


**Figure 7.**
*XRD spectra of pulsed laser deposited Orthorhombic $MoO_3$ and monoclinic $MoO_2$ thin films prepared at various deposition conditions.*

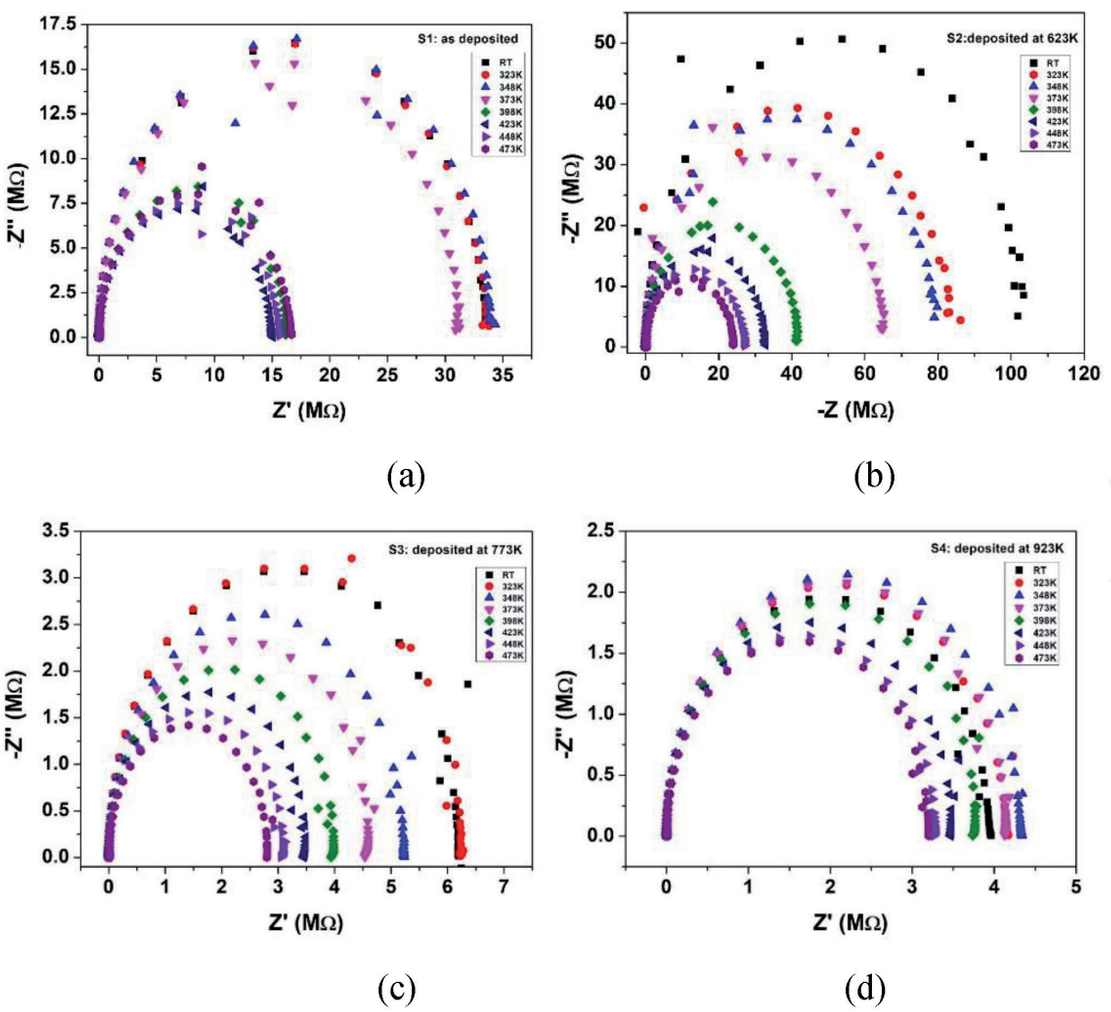


**Figure 8.**
*The complex impedance (Z" vs. Z') plots of ZMO thin films (a) 298 K (b) 623 K (c) 773 K and (d) 923 K.*

semicircles that are deformed and depressed with their centres below the real axis as the temperature range investigated, complex curve consists only one depressed semi-circle and its centre lies below the real axis. Furthermore, depressed arc is typical for a dipolar system involving distribution of relaxation time. Moreover, it is noted that the diameter of semi-circles decreases with increase in temperature which also refers to the decrease in the resistivity. The equivalent circuit for this sample is a series Resistor-Capacitor (RC) circuit. Whereas the semi-circled impedance samples possess the characteristics which are attributed to the semiconductor behaviour, in which the electrical conduction process is thermally activated.

The equivalent circuit for these depressed semi-circles of the ZMO thin films may be described by a parallel connection of an ohmic resistor R and a capacitor C, also known as Randles circuit. Here the capacitor is replaced with a constant phase element (CPE) associated with both the resistors and capacitors [12]. Indeed, in the present study, the complex plane plot can be described by the Nyquist plot, which is given by

$$Z = \frac{R}{\left[1 + (j\omega\tau)^{\alpha}\right]} \tag{2}$$

where ω is angular frequency, τ = RC is the relaxation time and α is a parameter that characterizes the distribution of relaxation times with values ranging from 0 to 1. When α is zero, the relaxation is said to be Debye relaxation and when α is greater than zero, the relaxation times are said to have distribution.

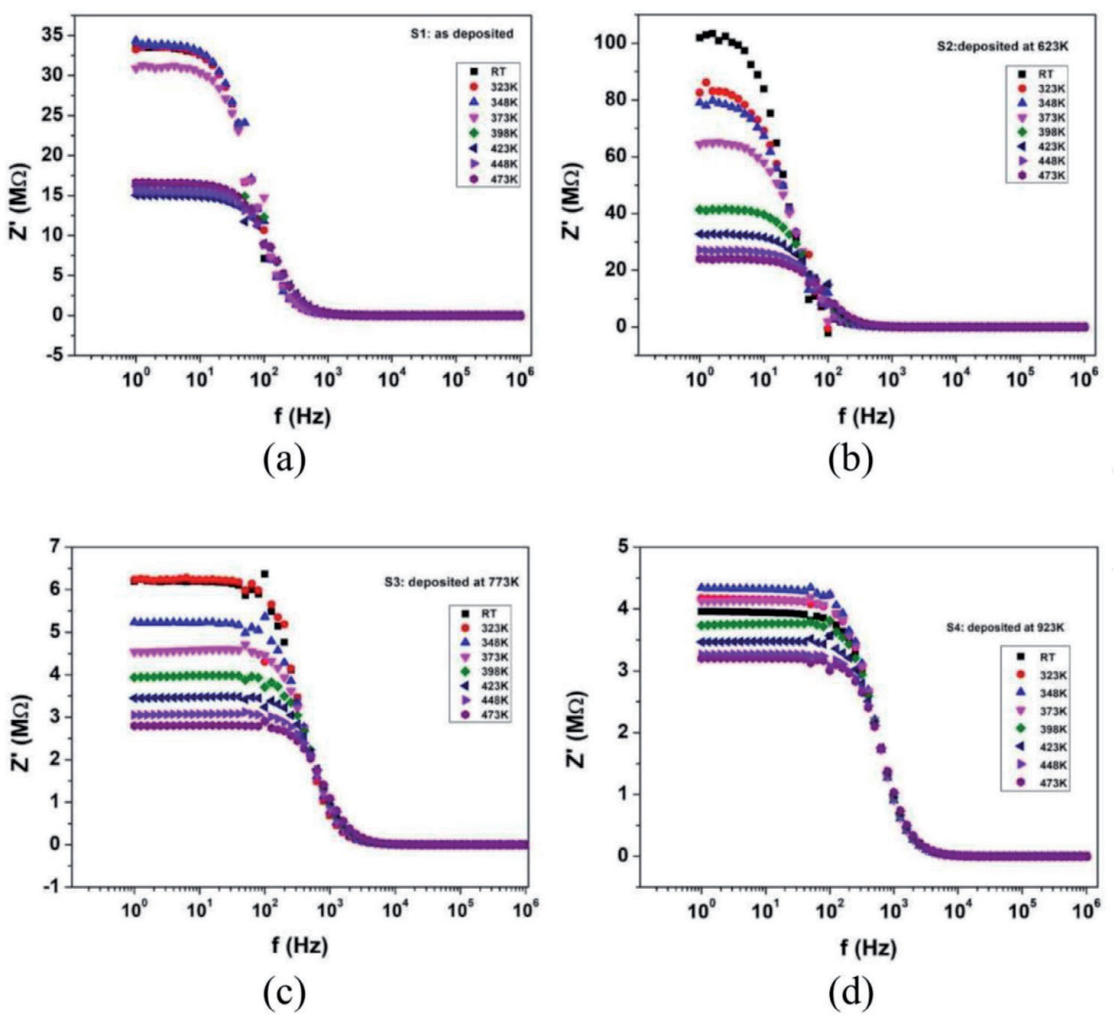


**Figure 9.**
*Frequency dependence of the real part (Z') of the complex impedance. (a) As deposited ZMO, (b) ZMO deposited at 623 K, (c) ZMO deposited at 773 K and (d) ZMO deposited at 923 K.*

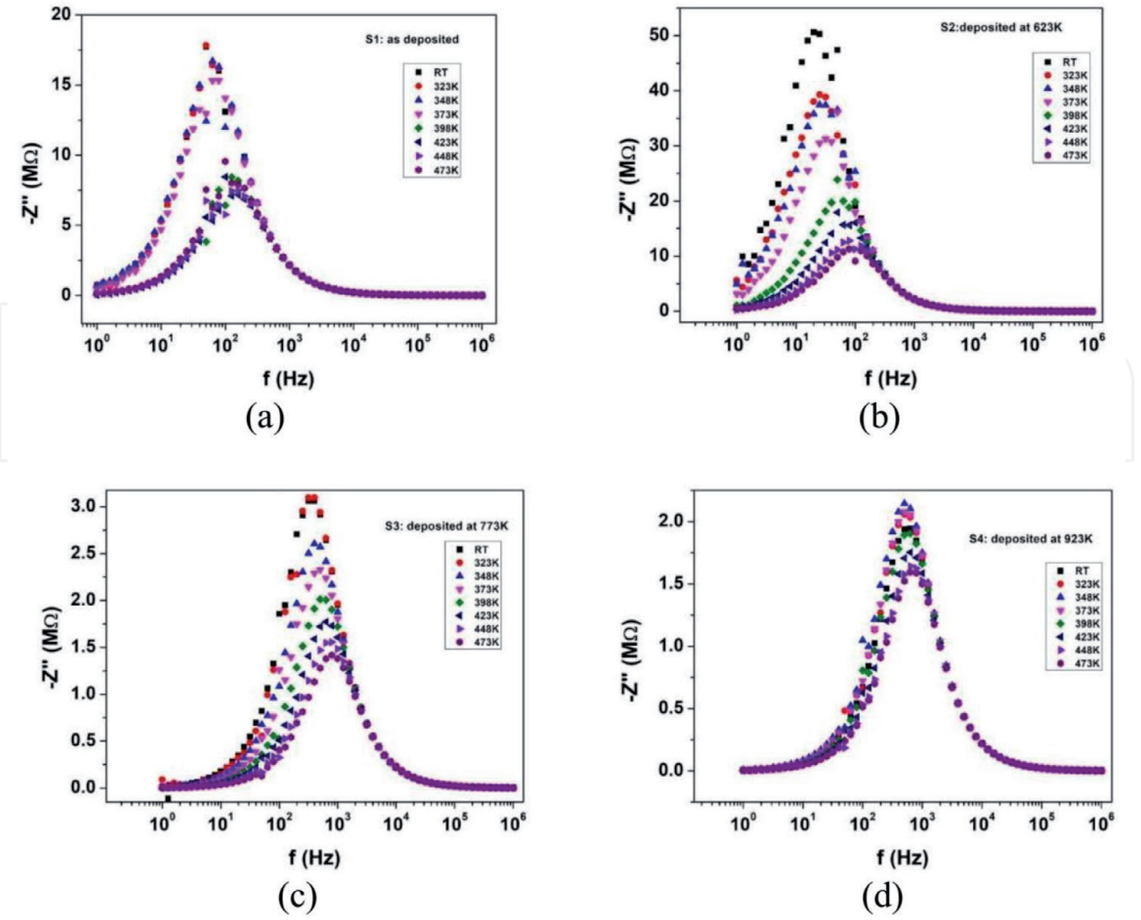


**Figure 10.**
*Imaginary part of impedance (Z") as a function of frequency. (a) As deposited ZMO, (b) ZMO deposited at 623 K, (c) ZMO deposited at 773 K and (d) ZMO deposited at 923 K.*

**Figure 9** shows the frequency dependence of the real part (Z') of the complex impedance Z* = Z'-jZ" for temperatures ranging from 298 K to 923 K [4].

It is observed that as there is a rise in the temperature and the frequency, the real impedance magnitude Z' decreases and hence the materials show a negative temperature coefficient of resistance (NTCR) and are attributed to a semiconductor behaviour. It is also noticed that the value of Z' for all the temperatures merges towards the high frequency due to the space charge dependent behaviour. The charge carriers are settled on the portion of the grain boundaries with sufficient energy to overcome the barrier with the increase in the temperature and hence we can emphasize as in conductivity. It can be seen that the peak position shifts from lower to higher frequencies with increasing temperatures. But the maximum value of the imaginary part $Z"_{max}$ values decreases due to thermally activated dielectric relaxation process as shown in **Figure 10** [4].

The same investigation carried out for the binary oxides $ZnO/V_2O_5$ and $ZnO/TiO_2$ and its performance as dielectric material with respect to wide frequency range and wide temperature range. The behaviour is compared and studied with respect to various deposition temperatures [13].

## 5. Conclusions

The nanostructured thin films metal oxides such as ZnO, $MoO_3$, $MoO_2$, binary oxides $ZnO/MoO_3$, $ZnO/TiO_2$ and $ZnO/V_2O_5$ were prepared using pulsed laser deposition technique. The ZnO thin film nanostructures are seen through the SEM/FESEM at the different deposition temperature. Through the increase of deposition

temperature to 450 °C, the orthorhombic $MoO_3$ and monoclinic $MoO_2$ are prepared at the $O_2$ and Ar gas deposition atmosphere and confirmed using the FESEM and XRD. The binary oxides $ZnO/MoO_3$, $ZnO/TiO_2$ and $ZnO/V_2O_5$ shows amorphous nature even at high deposition temperature. The thin films dielectric properties, electric modulus and impedance properties were analysed using ac complex impedance spectroscopy. The dielectric relaxation process is thermally activated for all the samples suitable for channel applications in FET devices. They confirm them to possess the nature of semiconducting property by the deformed semi-circle for the impedance Nyquist plots.



## Author details

Cyril Robinson Azariah John Chelliah[1*] and Rajesh Swaminathan[2]

1 Department of Nanotechnology, Institute of Electronics and Communication Engineering, Saveetha School of Engineering, Saveetha Institute of Medical and Technical Sciences, Saveetha University, Chennai, Tamil Nadu, India

2 Department of Physics, School of Sciences, Arts, Media and Management, Karunya Institute of Technology and Sciences, Coimbatore, Tamil Nadu, India

*Address all correspondence to: cyrilrobinsonazariahj.sse@saveetha.com

## References

[1] Rembert, T., Battaglia, C., Anders, A., & Javey, A. (2015)"Room Temperature Oxide Deposition Approach to Fully Transparent, All-Oxide Thin-Film Transistors", Advanced Materials, 27, 6090-6095.

[2] Babu, S. S., Moni, D. J., Padickala, P. J., Azariah, J. C. R., & Rajesh, S. (2018, March). Fabrication and Characterization of PLD Deposited Crystalline Zno as Channel and Amorphous Zno as Gate Dielectric of the Thin Film FET. In *2018 4th International Conference on Devices, Circuits and Systems (ICDCS)* (pp. 301-304). IEEE.

[3] Challam, A., Chelliah, C. R. A. J., Nirmal, D., & Swaminathan, R. (2018). Design and Fabrication of GaAs Based MOSFET by Physical Vapor Deposition Method. Materials Focus, *7*(4), 453-458.

[4] Chelliah, C. R. A. J., & Swaminathan, R. (2020). Enhanced Structural, Optical and Electrochemical Properties of Pulsed Laser Deposited Binary Zinc and Molybdenum Oxide Nanostructured Thin Films. In *Key Engineering Materials* (Vol. 853, pp. 68-72). Trans Tech Publications Ltd.

[5] Pandiyarajan T., Mangalaraja R.V., Karthikeyan B., Mansilla H.D., Gracia-Pinilla M.A. (2017) Spectroscopic Investigation on rGO:ZnO Composites Nanostructures. In: Ebenezar J. (eds) Recent Trends in Materials Science and Applications. Springer Proceedings in Physics, vol 189. Springer, Cham. https://doi.org/10.1007/978-3-319-44890-9_7

[6] Zhang, Yufei, Laiquan Li, Haiquan Su, Wei Huang, and Xiaochen Dong. "Binary metal oxide: advanced energy storage materials in supercapacitors." Journal of Materials Chemistry A 3, no. 1 (2015): 43-59.

[7] Chelliah, C. R. J., & Swaminathan, R. (2018). Pulsed laser deposited hexagonal wurzite ZnO thin-film nanostructures/nanotextures for nanophotonics applications. Journal of Nanophotonics, *12*(1), 016013.

[8] Chelliah, C. R. A. J., & Swaminathan, R. (2018). Study of the pulsed laser deposited ZnO thin films and its electrical performance as n-Channel in MOSFET. Journal of Nanoelectronics and Optoelectronics, *13*(5), 708-714.

[9] Kim, S. H., Badran, R. I., & Umar, A. (2017)"Fabrication of ZnO Nanorods Based p – n Heterojunction Diodes and Their Electrical Behavior with Temperature", Journal of Nanoelectronics and Optoelectronics, 12, 731-735.

[10] Chelliah, C. R. A. J., Ponmudi Selvan T., Samuel Rajasekar M., Sheebha, I., Vidhya, B., & Rajesh, S. (2018, March). Pulsed Laser Deposited Molybdenum Oxides (MoO 3 & MoO 2) Thin Films for Nanoelectronics Device Application. In *2018 4th International Conference on Devices, Circuits and Systems (ICDCS)* (pp. 42-47). IEEE.

[11] Balaji, M., Chandrasekaran, J., Raja, M., & Rajesh, S. (2016)"Structural, optical and electrical properties of Ru doped MoO3 thin films and its P–N diode application by JNS pyrolysis technique", Journal of Materials Science: Materials in Electronics, 27, 11646-11658.

[12] Ait Ahsaine H., Zbair M., Ezahri M., Benlhachemi A., Arab M., Bakiz B., Gavarri J.-R. (2015) "Rietveld refinements, impedance spectroscopy and phase transition of the polycrystalline ZnMoO4 ceramics", Ceramics International, 41, 15193-15201.

[13] Chelliah, C. R. A. J., & Swaminathan, R. (2019). Improved optical absorption, enhanced morphological and electrochemical properties of pulsed laser deposited binary zinc and vanadium oxide thin films. *Journal of Materials Science: Materials in Electronics*, 1-11.